Quad Performances and Manoeuvrability of TWQH platform

Achim IONITA*,[1], Andrei LUNGOCI*,[1], Ion TOMESCU*,[2]

*Corresponding author
[1]INCAS – National Institute for Aerospace Research "Elie Carafoli",
B-dul Iuliu Maniu 220, Bucharest 061126, Romania,
ionita.achim@incas.ro, lungoci.andrei@incas.ro
[2]Systems - Business Plus S.R.L.,
ion.tomescu@businessplus.ro

DOI: 10.13111/2066-8201.2022.14.4.6

Received: 23 August 2022/ Accepted: 22 September 2022/ Published: December 2022

Abstract: *Accurate dynamic modelling of the Tandem Wing Quadcopter Hybrid (TWQH) platform is becoming increasingly important, as strict requirements are progressively being imposed on the UAV (unmanned aerial vehicles) control system in the transition phase from vertical to level flight and vice versa. This work aims to present preliminary design performances in the steady and manoeuvring flight of the platform thrusted by only four rotors directed upward. The aerodynamic effects of tandem wings make a significant contribution to the evaluation of performance, controllability and manoeuvrability in hovering and low speed phase. More specifically, steady, level, symmetrical pull-up and coordinated turns approaches of the quad model are considered and the results obtained in the simulation study are presented and discussed.*

Key Words: *tandem wing, quadcopter, aerodynamic effects, flight performances, controllability, manoeuvrability*

LIST OF SYMBOLS

ρ, g, m (kg/m^3, m/sec^2, kg)	density of air, gravitational acceleration, mass
S, c, b (m^2, m)	reference area, aerodynamic chord, span
$\tilde{q}$ (kg/m/sec^2)	aerodynamic pressure
$I_{xx}, I_{yy}, I_{zz}, I_r$ (kgm^2)	main inertial moments of vehicles, inertia moment of propellers
$\overline{V}$, $\overline{\Omega}$, $\overline{\omega}$	velocity vector, angular velocity vector and Euler angles vector on the Oxyz frame
$\overline{M_T}$	moment vector due to thrust
$\overline{h_r}$	gyroscopic vector moment due to rotors
$\overline{F_T}$	forces vector to thrust
$\overline{F_G}$	gravitational vector
$\bar{x}$	position vector on the Oxyz frame
C	rotation matrix
$\bar{B}$	transformation matrix for angular velocities
X, Y, Z (N)	aerodynamic forces on Oxyz frame
U_1, U_2, U_3, U_4 (N)	control variables due to electric motors
$\dot{u}$,$\dot{v}$, $\dot{w}$ [m/sec^2]	linear acceleration

$\dot{p}, \dot{q}, \dot{r}$ [rad/sec^2]	angular accelerations
$\dot{\varphi}, \dot{\theta}, \dot{\psi}$ [rad/sec]	angular velocities
c_f, c_q $N/(rad/\sec)^2$, $Nm/(rad/\sec)^2$	strength and moment coefficients
a, b, l (m)	distances between rotors and centre of gravity
ω_i , Ω_r (rpm or rad/sec)	rotor speed (*i =1,2,3,4*)
ω_n, ω_t, n (deg/sec, -)	load turn rate, sustained turn rate, load factor
u, v, w $(m/\sec)$	body velocities
p, q, r (rad/sec)	body angular rates
φ, θ, ψ $(\deg or\ rad)$	Euler angles
α, β, γ $(\deg or\ rad)$	angle of attack, sideslip, flight path angles
z_E (m)	altitude
D_A, L_A, Y_A (N)	drag, lift and side force in stability axes frame
$\mathcal{L}_A, \mathcal{M}_A, \mathcal{N}_A$ (Nm)	roll, pitch, yaw moments in body axes frame
C_D, C_Y, C_L	drag, side force, and lift aerodynamic coefficients
$C_{D_0}, C_{L_0}, C_{m_0}$	drag, lift and pitch moment coefficients at zero lift coefficient
C_{L_α}, C_{L_q}	derivative of the lift coefficient in respect of the incidence and pitch rate
C_{m_α}, C_{m_q}	derivative of pitch moment in respect of the incidence and pitch rate
$C_{Y_\beta}, C_{Y_p}, C_{Y_r}$	derivative of side force coefficient in respect of the sideslip, roll and yaw rates
$C_{l_\beta}, C_{l_p}, C_{l_r}$	derivative of rolling moment in respect of the sideslip, roll and yaw rates
$C_{n_\beta}, C_{n_p}, C_{n_r}$	derivative of yawing moment in respect of the sideslip, roll and yaw rates

1. INTRODUCTION

Recent developments in electric propulsion systems, high storage batteries, miniaturizing equipment and nonlinear techniques have shown that unmanned aerial vehicles (UAV) already have a wide range of possible applications in both civil and military fields, due to reduced manufacturing costs as well as operational costs, compared to piloted vehicles. Their potential uses are diversified, including border patrol missions, search, and fire monitoring and road traffic [1]. Generally, UAVs are preferred for dangerous and pilot effort/ long-range pilot missions. Most of the aforementioned missions require vertical take-off and landing (VTOL). The TWQH (Tandem Wing Quadcopter Hybrid) configuration offers an alternative in executing typical flight phases specific to fixed-wing vehicles (long distance flights, tracking, mapping, inspection, search and rescue) as well as to vehicles with rotary wing (hovering, VTOL, monitoring, identification).

According to our analysis, no systematic modelling work has been documented in the literature on dual system such as TWQH [2]. This has a different dynamics, aerodynamics and actuation, and therefore, is different in the mode of operation. The main goal of this work is to analyse some unique features of the hybrid platform with different orientations of thrust. These results should be taken into account in order to develop a controller aiming to achieve a transition flight from hover to cruise mode and vice versa because a safe transition between different phases is essential. The numerical simulations for the TWQH dynamics regarding the performances and driveability suggest that the hybrid configuration driven by four electric rotors will reach different limitations on flight performances with respect to the performances obtained for tandem wing airplanes driven by thermal engines.

2. MOTIVATION AND OBJECTIVES

An experimental prototype named Tandem Wing Quadcopter Hybrid was developed to perform vertical and level flight (fig. 1). This TWQH combines the high-speed cruise capabilities of a conventional aircraft with hovering capabilities of a quadcopter. The vehicle is driven by a thermic engine for cruise and four electric motors for VTOL phases. This platform has an additional structure in the tandem wing, aligned parallel to the fuselage which has four electric motors, vertically aligned, used for hovering. Due to this specific design, we distinguish three operational configurations: that as a rotary wing platform (QH) when the hybrid is driven only by upward motors, that as a hybrid platform (TWQH) for transition with all engines activated and that as a conventional airplane (TW) when using only pusher thermal engine [3]. In level flight for TW the elevator, aileron/ flaps and rudder are taken into account. The TWQH is designed with rotors mounted near each wing tip. Thus, the wing airflow is affected by the aerodynamic interference due to the rotors down washing which, consequently, will modify the aerodynamic characteristics of the tandem wings and control surfaces (aileron and elevator), making flight control more difficult. With respect to other UAV vehicles, the TWQH hybrid is a dual system which has a simple mechanism and control, providing a smooth transition, enhancing vertical flight, stability, controllability, easy take-off and landing [4, 5].

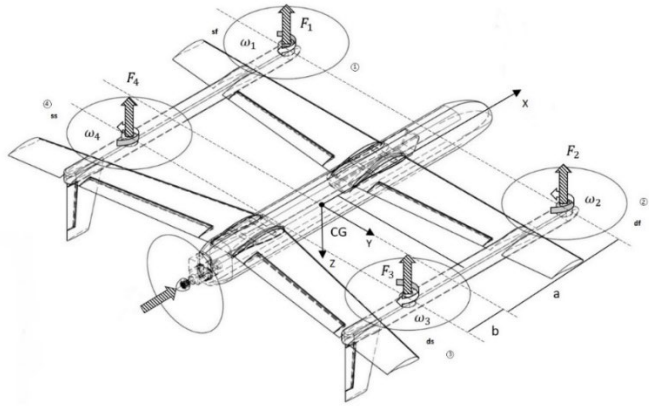

Fig. 1 – Experimental prototype

This paper proposes a qualitative analyse of the main flight phases such steady, level, symmetrical pull-up and coordinated turns in preliminary design of the hybrid vehicle driven by upward rotors (QH), in order to configure the controller characteristics for the transition phase. The flight speed domain considered for the TW configuration in this work is between 18 m/sec (stalling speed in approach) and over 40 m/sec (cruising speed with 75% max. continuous power). During the transition phase from QH mode to TW mode and back (where the hybrid vehicle encounters a large variation of incidence angle), a translational speed between 18 and 24 m/sec is assumed. The TWQH platform enclosed in class I small MALE (Medium Altitude Long Endurance Air Vehicle) according to [6].

Performance characteristics on QH in various flight phases will be determined by analysing the nature of forces and moments generated by the quadrotors vector and the aerodynamic contribution that act on the vehicle in a steady state condition of level flight, climb or turn. The main elements of the vehicle performance are determined by the power requirements, the distances from the centre of the rotors to the the centre of gravity and the

propeller strength and torque coefficients in steady flight at a uniform speed. Changing the position of the power vector (rotors pointing upwards) affects the airplane performance, controllability and manoeuvres at any given speed and altitude. Extensive knowledge of the dynamic model is needed. The transition phase sometimes suffers from the lack of controllability. Our goal is to develop a dynamic model including all flight regimes to increase the performance of the control law and to assure a smooth transition between QH and TW modes. A decoupling mechanism is strongly needed in the transition manoeuvre. This must be implemented in the control allocation algorithm as a function of speed where the angular rotor speed and the surface deflection are often mixed together [7]. The challenge is to extend the control envelope for the 6DoF nonlinear model of TWQH to all operational regimes.

3. STATE SPACE MODEL

The mathematical model presented below describes the TWQH movement and behaviour with respect to the initial input values of the model and external influences on the vehicle. The TWQH frame with only four propellers is the component that will be taken into account in these dynamics. The TWQH design with corresponding angular velocities for the quad configuration is presented in fig. 1.

The equations of motion for the TWQH configuration are those applied in flight mechanics, which are detailed in the works of Etkin [8], Hacker [9], Roskam [10] applied to a UAV vehicle in which the thrust vector includes the fixed wing component such as the rotary wing component. The quadrotor motion is caused by a series of moments due to body and propeller gyro effects. The state-space model has been developed in [11].

The dynamic model of this hybrid is derived in both vertical and horizontal flight mode using the Newton - Euler approach. It requires the defintion of two reference frames: one is an inertial reference frame and the other is a body reference frame, originating in the vehicle's centre of gravity (shown in Fig. 1). Here we assume that the Ox axis is aligned with the direction of the thermal thrust engine. In order to continue with the development of the model, it is worth mentioning the following assumption:

- the TWQH platform is a rigid body,
- the TWQH structure is assumed to be symmetric,
- the neutral point of aerodynamic configuration is behind the center of gravity,
- the aerodynamic contribution of surface control is neglected,
- the thrust components are proportional to the square of the propeller speed,
- the gyroscopic effect due to the rotation of the propeller is taken into account,
- the response of electric motors to propellers is assumed to be instantaneous,
- the propeller-wing interaction is neglected in this phase.

Let Oxyz be a body-fixed frame whose origin is at the centre of mass (CoM). The absolute position of QH is defined by the position (x, y, z) and the attitude defined by the Euler angles. The QH dynamics uses the Newton – Euler method expressed by differential equations as follows:

$$m(\dot{\overline{V}} + skew(\Omega) \cdot \overline{V}) = \overline{F_G} + \overline{F_T} + \overline{F_A} \tag{1}$$

$$\dot{\bar{x}} = C\overline{\mathrm{V}} \tag{2}$$

$$I\dot{\overline{\Omega}} + \dot{\overline{h_r}} + skew(\Omega)\left(I \cdot \overline{\Omega} + \overline{h_r}\right) = \overline{M_T} + \overline{M_A} \tag{3}$$

$$\dot{\bar{\omega}} = B^{-1}\overline{\Omega} \tag{4}$$

where the components are defined as follows:

$$\bar{V}=\begin{pmatrix}u\\v\\w\end{pmatrix}\quad \overline{F_G}=C\cdot\begin{pmatrix}0\\0\\mg\end{pmatrix}\quad \overline{F_T}=\begin{pmatrix}0\\0\\U_1\end{pmatrix}\quad \overline{F_A}=\begin{pmatrix}X_A\\Y_A\\Z_A\end{pmatrix}\quad \bar{x}=\begin{pmatrix}x\\y\\z\end{pmatrix}$$

$$\overline{\Omega}=\begin{pmatrix}p\\q\\r\end{pmatrix}\quad \overline{\omega}=\begin{pmatrix}\varphi\\\theta\\\psi\end{pmatrix}\quad skew(\Omega)=\begin{pmatrix}0&-r&q\\r&0&-p\\-q&p&0\end{pmatrix} \tag{5}$$

$$\overline{M_T}=\begin{pmatrix}U_2\\U_3\\U_4\end{pmatrix}\quad \overline{M_A}=\begin{pmatrix}\mathcal{L}_A\\\mathcal{M}_A\\\mathcal{N}_A\end{pmatrix}\quad \overline{h_r}=\begin{pmatrix}h_{rx}\\h_{ry}\\h_{rz}\end{pmatrix}\quad I=\begin{pmatrix}I_{xx}&0&0\\0&I_{yy}&0\\0&0&I_{zz}\end{pmatrix}$$

$$C=\begin{pmatrix}\cos\psi\cos\theta & \sin\varphi\sin\theta\cos\psi-\cos\varphi\sin\psi & \cos\varphi\sin\theta\cos\psi+\sin\varphi\sin\psi\\ \sin\psi\cos\theta & \sin\varphi\sin\theta\sin\psi+\cos\varphi\cos\psi & \cos\varphi\sin\theta\sin\psi-\sin\varphi\cos\psi\\ -\sin\theta & \sin\varphi\cos\theta & \cos\varphi\cos\theta\end{pmatrix} \tag{6}$$

$$B=\begin{pmatrix}1&0&-\sin\theta\\0&\cos\varphi&\cos\theta\sin\varphi\\0&-\sin\varphi&\cos\theta\cos\varphi\end{pmatrix} \tag{7}$$

The gyroscopic effect due to the rotation of the propulsion unit is kept only for the Oz axis, $h_{rx}=0$, $h_{ry}=0$ and $h_{rz}\approx I_r\Omega_r$

The system that defines the movement of the quadcopter includes the following states and control variables:

- the state variables are: $(u,v,w,p,q,r,\varphi,\theta,\psi,z)$,
- the control variables are: (U_1,U_2,U_3,U_4)

The translation, rotational and kinematic equations describing the dynamics of the QH configuration with respect to the body axes frame are:

$$\dot{u}=rv-qw-gsin\theta+i_1X \tag{8}$$

$$\dot{v}=pw-ru+gcos\theta sin\varphi+i_1Y \tag{9}$$

$$\dot{w}=qu-pv+gcos\theta cos\varphi+i_1Z-i_1U_1 \tag{10}$$

$$\dot{p}=i_5qr+i_2\mathcal{L}_A-i_8q+i_2U_2 \tag{11}$$

$$\dot{q}=i_6rp+i_3\mathcal{M}_A+i_9p+i_3U_3 \tag{12}$$

$$\dot{r}=i_7pq+i_4\mathcal{N}_A+i_4U_4 \tag{13}$$

$$\dot{\varphi}=p+qsin\varphi tan\theta+rtan\theta cos\varphi \tag{14}$$

$$\dot{\theta}=qcos\varphi-rsin\varphi \tag{15}$$

$$\dot{\psi}=q\frac{sin\varphi}{cos\theta}+r\frac{cos\varphi}{cos\theta} \tag{16}$$

Aditionally from (2), we retain:

$$\dot{z_E}=V(sin\alpha cos\beta cos\phi cos\theta-cos\alpha cos\beta sin\theta+sin\beta sin\phi cos\theta) \tag{17}$$

with

$$\theta=\alpha+\gamma \tag{18}$$

The aerodynamic forces and moments of the TQWH make an important contribution to estimating the performance of the QH configuration. This includes the contribution of rotational motion variables p, q, r involved in the steady manoeuvring flight (pulling-up and turning). In addition to the body axes equation, it is important to express the aerodynamic forces and moments in the axes of stability; because they act here with V, angle of attack α can be expressed in terms of u and w. The aerodynamic coefficients are assumed to be independent of flight speed. In this way, the aerodynamic forces in terms of lift, drag, and side force expressed in the stability-axis system are [8]:

$$\begin{aligned} D_A &= \tilde{q}SC_D = \tilde{q}S\left[C_{D_0} + K \cdot {C_L}^2\right] \\ Y_A &= \tilde{q}SC_Y = \tilde{q}S\left[C_{Y_\beta} \cdot \beta + \left(C_{Y_r} r + C_{Y_p} p\right) \cdot \frac{b}{2 \cdot V}\right] \\ L_A &= \tilde{q}SC_L = \tilde{q}S\left[C_{L_0} + C_{L_\alpha} \cdot \alpha + C_{L_q} q \frac{c}{2 \cdot V}\right] \end{aligned} \tag{19}$$

and

$$\begin{aligned} \mathcal{L}_A &== \tilde{q}Sb\left[C_{l_\beta}\beta + \left(C_{l_r} r + C_{l_p} p\right)\frac{b}{2 \cdot V}\right] \\ \mathcal{M}_A &= \tilde{q}Sc\left[C_{m_0} + C_{m_\alpha} \cdot \alpha + C_{m_q} q \frac{c}{2 \cdot V}\right] \\ N_A &= \tilde{q}Sb\left[C_{n_\beta}\beta + \left(C_{n_r} r + C_{n_p} p\right)\frac{b}{2 \cdot V}\right] \end{aligned} \tag{20}$$

where:

$$V = \sqrt{u^2 + v^2 + w^2} \tag{21}$$

with

$$\begin{aligned} u &= V cos\alpha cos\beta \\ v &= V sin\beta \\ w &= V sin\alpha cos\beta \end{aligned} \tag{22}$$

and aerodynamic pressure

$$\tilde{q} = \frac{\rho V^2}{2} \tag{23}$$

Between the components of the aerodynamic forces in the body axes system and the aerodynamic forces in the stability axes system we have the following relation:

$$\begin{pmatrix} X \\ Y \\ Z \end{pmatrix} = \begin{pmatrix} cos\alpha cos\beta & sin\beta & sin\alpha cos\beta \\ -cos\alpha sin\beta & \cos\beta & -sin\alpha sin\beta \\ -sin\alpha & 0 & cos\alpha \end{pmatrix} \begin{pmatrix} -D_A \\ -Y_A \\ -L_A \end{pmatrix} \tag{24}$$

Usually, we prefer to express the components X and Z as function of D_A, L_A and Y.

$$X = -\frac{D_A cos\alpha}{cos\beta} - Y cos\alpha tan\beta + L_A sin\alpha \tag{24a}$$

$$Z = -\frac{D_A sin\alpha}{cos\beta} - Y sin\alpha tan\beta - L_A cos\alpha \tag{24c}$$

Here, with small angles of sideslip, we assume:

$$Y = -D_A sin\beta - Y_A cos\beta \approx Y_A \tag{24b}$$

The following notations are made:

$$\begin{gathered} i_1 = \frac{1}{m};\quad i_2 = \frac{1}{I_{xx}};\quad i_3 = \frac{1}{I_{yy}};\quad i_4 = \frac{1}{I_{zz}};\quad i_5 = \frac{I_{yy} - I_{zz}}{I_{xx}}; \\ i_6 = \frac{I_{zz} - I_{xx}}{I_{yy}};\quad i_7 = \frac{I_{xx} - I_{yy}}{I_{zz}};\quad i_8 = \frac{I_r \Omega_r}{I_{xx}};\quad i_9 = \frac{I_r \Omega_r}{I_{yy}} \end{gathered} \tag{25}$$

where:

$$\Omega_r \approx (\omega_1 - \omega_2 + \omega_3 - \omega_4) \tag{26}$$

Total thrust produced by the four rotors in free air is:

$$U_1 = c_f(\omega_1^2 + \omega_2^2 + \omega_3^2 + \omega_4^2) \tag{27}$$

The control torque with respect to Oxyz frame generated by the four rotors is:

$$U_2 = c_f l(\omega_1^2 - \omega_2^2 - \omega_3^2 + \omega_4^2) \tag{28}$$

$$U_3 = c_f[a(\omega_1^2 + \omega_2^2) - b(\omega_3^2 + \omega_4^2)] \tag{29}$$

$$U_4 = c_q(\omega_1^2 - \omega_2^2 + \omega_3^2 - \omega_4^2) \tag{30}$$

The Inverted movement matrix for the rotor speeds is used to calculate the squared angular propeller's velocities that input the variables as follows:

$$\omega_1^2 = \frac{1}{4(a+b)}\left(\frac{2b}{c_f}U_1 + \frac{a+b}{c_f l}U_2 + \frac{2}{c_f}U_3 + \frac{a+b}{c_M}U_4\right) \tag{31}$$

$$\omega_2^2 = \frac{1}{4(a+b)}\left(\frac{2b}{c_f}U_1 - \frac{a+b}{c_f l}U_2 + \frac{2}{c_f}U_3 - \frac{a+b}{c_M}U_4\right) \tag{32}$$

$$\omega_3^2 = \frac{1}{4(a+b)}\left(\frac{2a}{c_f}U_1 - \frac{a+b}{c_f l}U_2 - \frac{2}{c_f}U_3 + \frac{a+b}{c_M}U_4\right) \tag{33}$$

$$\omega_4^2 = \frac{1}{4(a+b)}\left(\frac{2a}{c_f}U_1 + \frac{a+b}{c_f l}U_2 - \frac{2}{c_f}U_3 - \frac{a+b}{c_M}U_4\right) \tag{34}$$

4. STEADY STATE PERFORMANCE OF THE QUAD HYBRID CONFIGURATION

The trim condition of the aircraft is a combination of state and control inputs for which the forces and moments are in equilibrium and at the same time satisfy a given flight condition

$$X(x,u) = 0 \tag{35}$$

In short, from equation (8 – 16) for the general motion, the kinematic constrains for trimmed flight are derived. They are discussed separately for each flight phase. Steady motion requires

$$\dot{\vec{V}} = \begin{pmatrix} \dot{u} \\ \dot{v} \\ \dot{w} \end{pmatrix} = 0, \qquad \dot{\vec{\Omega}} = \begin{pmatrix} \dot{p} \\ \dot{q} \\ \dot{r} \end{pmatrix} = 0, \quad \dot{\vec{\omega}} = \begin{pmatrix} \dot{\varphi} \\ \dot{\theta} \\ \dot{\psi} \end{pmatrix} = 0 \tag{36}$$

These conditions lead to the following set of equilibrium equations (the subscripts of variables show the trim conditions):

$$r_0 v_0 - q_0 w_0 - g sin\theta_0 + i_1 X = 0 \tag{8a}$$

$$p_0 w_0 - r_0 u_0 + g cos\theta_0 sin\varphi_0 + i_1 Y = 0 \tag{9a}$$

$$q_0 u_0 - p_0 v_0 + g cos\theta_0 cos\varphi_0 + i_1 Z - i_1 U_1 = 0 \tag{10a}$$

$$i_5 q_0 r_0 + i_2 \mathcal{L}_A = -i_8 q_0 + i_2 U_2 = 0 \tag{11a}$$

$$i_6 r_0 p_0 + i_3 \mathcal{M}_A + i_9 p_0 + i_3 U_3 = 0 \tag{12a}$$

$$i_7 p_0 q_0 + i_4 \mathcal{N}_A + i_4 U_4 = 0 \tag{13a}$$

$$p_0 + q_0 sin\varphi_0 tan\theta_0 + r_0 tan\theta_0 cos\varphi_0 = 0 \tag{14a}$$

$$q_0 cos\varphi_0 - r_0 sin\varphi_0 = 0 \tag{15a}$$

$$q_0 \frac{sin\varphi_0}{cos\theta_0} + r_0 \frac{cos\varphi_0}{cos\theta_0} = 0 \tag{16a}$$

$$sin\alpha_0 cos\beta_0 cos\varphi_0 cos\theta_0 - cos\alpha_0 cos\beta_0 sin\theta_0 + sin\beta_0 sin\varphi_0 cos\theta_0 + sin\gamma_0 = 0 \tag{17a}$$

Using equations (8a – 17a) and constrains defined by the TWQH aerodynamic configuration and propeller dynamics, we obtain the control inputs at any arbitrary flight condition.

5. STUDY CASES

For simulation purposes, we will use the flight vehicle data from [3, 11, 12]. From a control design perspective, this evaluation is useful to obtain a set of operating points for which there is a feasible speed of rotor. This work is used to generate some envelopes around the stalling speed of the TW configuration. Performance and manoeuvrability are degraded when operating near the extreme points of angular speed of rotors. The flight conditions strongly depend on the ω_i domain. Second, the manoeuvrability of the QH configuration is analysed to estimate the coupling effects and agility of the hybrid vehicle. The rotating speed of propellers domain translates into vehicle state-space limitation in the form of a feasible flight envelope in which stability and controllability of motion are possible. The control variables are a function of squared angular velocities for different RPMs (route per minute). The trim point analysis is used to generate a reference for the control approach. The behaviour of the mathematical model controls is dependent on the input values. The output values are chosen to be the limits of the first value of ω_i that exceeds the propeller domain. Based on the given and calculated values that are needed to compute the output values, we obtain the envelopes for which the TWQH will behave in expected way. In all cases, the altitude is kept constant.

5.1 Un-accelerated flight

It is assumed that the TWQH vehicle does not have angular body speeds. Only steady state and straight line flight are considered.

5.1.1 Symmetrical level flight

For steady, symmetrical powered flight the equations of motion considered here are (8 – 10). The initial conditions for steady state powered straight line flight are:

$$u= u_0;\ w= w_0;\ z= z_0;\ \alpha= \alpha_0;\ U_2(\omega_i) = 0 \quad U_4(\omega_i) = 0$$

In all cases, the equations that describe the symmetrical level motion are 8a, 10a, 12a and 22a.

5.1.1.1 forward/ backward

In the level flight case at γ=0 we assume that the conditions of equilibrium are reduced at equation 8, 10 and 12 from which we obtain the required control values:

$$U_1(\omega_i)^2 \pm 2U_1(\omega_i)Z(\alpha_0,V) + X(\alpha_0,V)^2 + Z(\alpha_0,V)^2 - (mg)^2 = 0 \tag{37}$$

where true values are for $U_1(\omega_i) > 0$, and

$$U_3(\omega_i) = -\mathcal{M}_A(\alpha_0,V) \tag{38}$$

We note that the positive second term in eq. 37 corresponds to forward flight and the negative sign is atribuited to backward flight.

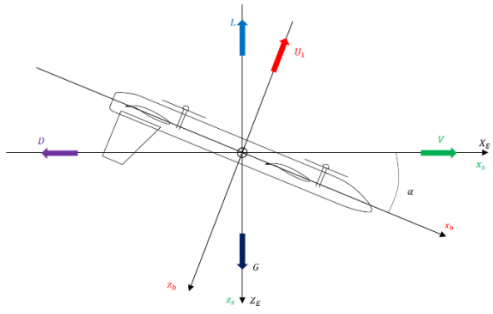

Fig. 2 – Forward flight ($\alpha_0 < 0$)

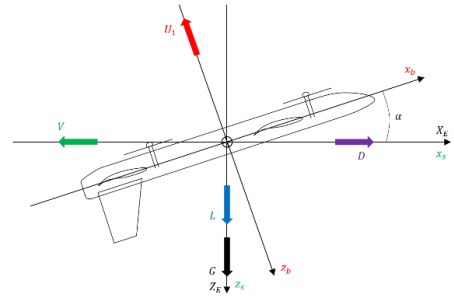

Fig. 3 – Backward flight ($\alpha_0 > 0$)

Note – The biggest weakness in symmetrical level backward flight is that the aerodynamic forces and moments become strongly nonlinear. The way to verify this motion is to do a flight experiment to check the limits of the envelope. Although on the low angle of attack range (+ 5 degrees), we assume that the lifting force is linear. The lifting force and the pitch moment change their sign. The neutral point is positioned behind the centre of gravity in the direction of movement. A rough estimate of this motion shows that a backward flight of up to 10 m/sec is possible. The U_3 control with the condition a < b has the ability to counteract the aerodynamic effect of the aerodynamic moment of the tandem wing. The flight tests may or may not confirm these assumptions.

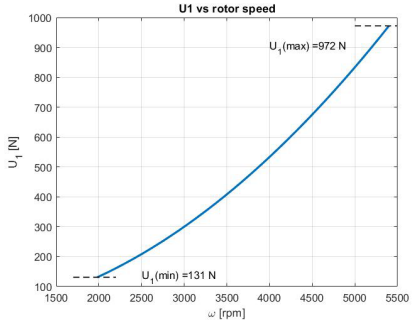

Fig. 4 – Available thrust control

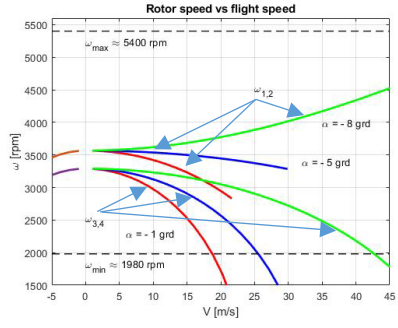

Fig. 5 – Rotor speed rates for different velocities

Fig. 5 shows that the high value of the QH forward speed corresponds to the cruising speed of the TW configuration and this decrease when the incidence becomes low.

5.1.1.2 climb/ descent flight

In the climb flight case with $\gamma \neq 0$ the conditions for equilibrium are obtained in the same way as described above:

$$U_1(\omega_i) = \frac{X(\alpha_0, V)}{tg\theta_0} + Z(\alpha_0, V) \tag{39}$$

with $tg\theta_0 \neq 0$

The forces acting on the TWQH in flight with $\gamma \neq 0$ are depicted in figures 6, 7.

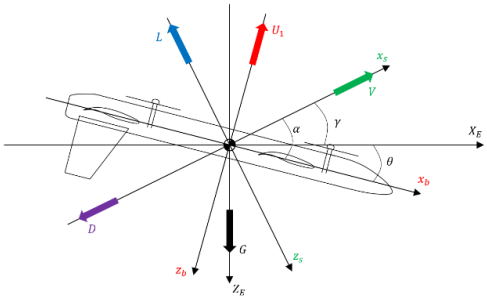

Fig. 6 – Climb

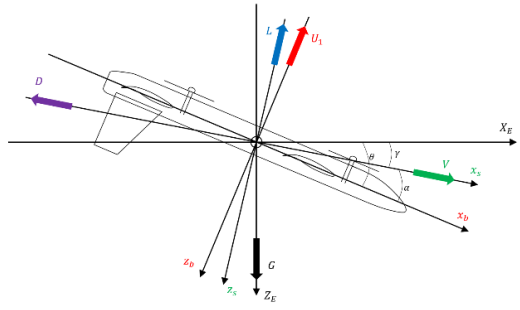

Fig. 7 – Descent

The behaviour of the TWQH is shown in figure 8, taking into account the available thrust:

$$\gamma = atan\frac{X(\alpha_0, V)}{U_1(\omega_i) - Z(\alpha_0, V)} - \alpha \tag{40}$$

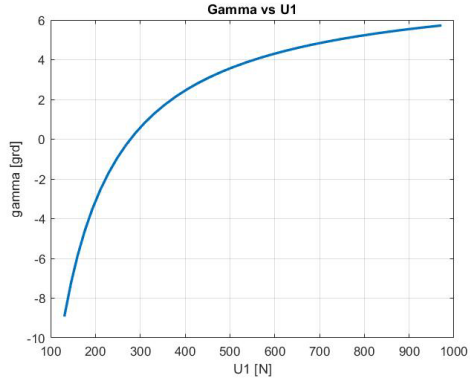

Fig. 8 – Flighpath angle as a function of available thrust

The flight is possible only with small flight path angles.

5.1.1.3 vertical ascent/ descent (VTOL)

In the case of hovering mode and VTOL phases with α_0=0, all four propellers had the same RPM. Equations 8 and 10 lead to:

$$w = \sqrt{2\frac{|U_1(\omega_i) - mg|}{\rho S C_D^*}} \tag{41}$$

where

$$w > 0 \qquad U_1 > mg$$

$$w < 0 \qquad U_1 < mg$$

and assuming

$$\mathcal{M}_A(\alpha_0, V) \approx 0 \quad \rightarrow \quad U_3(\omega_i) = 0$$

The distribution of the thrust in vertical motion strongly depends of the distances between the rotors and the centre of gravity where $\lambda = \frac{a}{b}$ is an important design parameter:

$$\frac{\omega_3^2 + \omega_4^2}{\omega_1^2 + \omega_2^2} \approx \frac{a}{b} \tag{42}$$

If we analyze separatly the lift contribution of the tandem wing for equilibrium in VTOL flight, the results on the pitch moment are similar.

We assume a drag area coefficient $SC_D^* \approx 2 * 1.125$ ($b^2/S \approx 0.48$) with Reynolds number between 10^4 and 10^6 (tandem wings considered as plate shape [13]). In hovering, we have:

$$\omega_{w=0} = \frac{1}{2}\sqrt{\frac{mg}{c_f}} \tag{43}$$

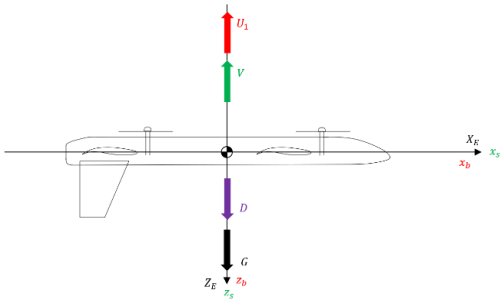

Fig. 9 – Ascent flight (VTOL, $\alpha_0 = 0$), $U_1 > mg$

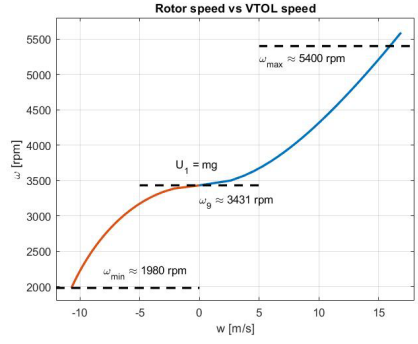

Fig. 10 –vertical speed function as propeller speed

The vertical speed depends on the available thrust/required thrust ratio and the limits of the rotor rates (see fig. 10).

5.1.2 lateral directional (steady side-slipping) flight

In the case of lateral directional motion with initial conditions:

$$u = u_0 \,;\; v = v_0 \,;\; \alpha = \alpha_0 ;\; \gamma = 0;$$

and parameter:

$$\beta = 0 \div \beta_{max} \;\;,$$

we will get the values for bank angle and velocity domains.

At a given bank angle in the steady state stright line from equations 9a,11a and 13a the available thrust is obtained to perform motion:

$$U_1(\omega_i)^2 - 2U_1(\omega_i)Z(\alpha_0, V) + X(\alpha_0, V)^2 + Y(\beta, V)^2 + Z(\alpha_0, V)^2 - (mg)^2 = 0 \tag{44}$$

where true values for $U_1(\omega_i) > 0$
and the bank angle can be obtained:

$$\varphi = \text{asin}\left(\frac{-Y_A(\beta,V)}{mgcos(\alpha_0)}\right) \tag{45}$$

The yawing and rolling torques are exceeded by the U_2 and U_4 controls corresponding to asymetric propellers on each side of the fuselge in respect with the sideslip angle:

$$U_2(\omega_i) = -\mathcal{L}_A(\beta,V) \quad U_3(\omega_i) = -\mathcal{M}_A(\alpha_0,V) \quad U_4(\omega_i) = -\mathcal{N}_A(\beta,V) \tag{46}$$

The numerical estimation obtained from equations 44 through 46 are considered to be acceptable up to sideslip angle $\beta = \pm 20$ deg.

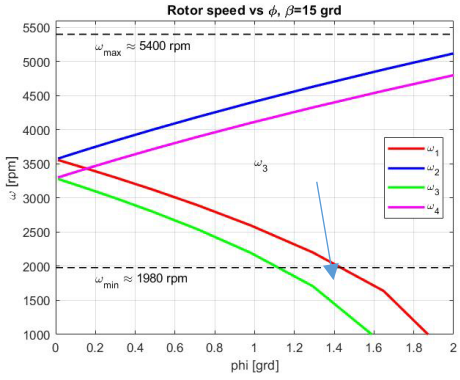

Fig. 11 – Bank angle function as propeller speed

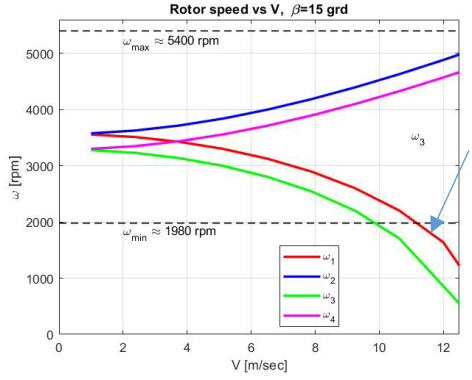

Fig. 12 – Velocity function as propeller speed

Figure 11 represents the available propeller thrust as a function of bank angle and figure 12 illustrates the maximum speed at which TWQH can be controlled. The bank angles are small and are not influenced by the incidence.

5.2 Manoeuvring flight

In this case, the angular velocity of hybrid platform may have a nonzero value. The resultant angular velocity of the airplane is:

$$p=p_0;\ q=q_0;\ r=r_0;$$

The manoeuvring (V-n manoeuvre diagram) and flight envelopes provide limits for flight velocity, turn speed and limit loads factor. The recommendation for UAV takes into account the relatively low flight speed and low loads factors [4]. Our analyses assume a structural limit $n_{Zmax} = +3.8$ for fixed-wing TH [11] and $\alpha_0 = ct$. The aerodynamic forces take into account the angular rates (p_0, q_0, r_0) and also the gyroscopic effect of the rotors is included in the estimate.

5.2.1 steady-symmetrical sustained pull-up maneouver

The numerical simulation is performed with the following initial conditions:

$$V = V_0;\ u= u_0;\ w=w_0;\ \alpha= \alpha_0;\ q=q_0;$$

and

$$U_2(\omega_i) = 0,\ U_4(\omega_i) = 0;$$

$$q_0 = \frac{g}{V_0}(n-1) \tag{47}$$

from equations 8a,10a and 12a it is obtained the available thrust to perform motion:

$$w_0 = \frac{1}{q_0}[-g\sin\theta + i_1 X(\alpha_0, q_0, V)] \tag{48}$$

$$u_0 = \sqrt{V_0^2 - w_0^2} \tag{49}$$

$$U_1(\omega_i) = \frac{1}{i_1}(q_0 u_0 + g\cos\theta) + X(\alpha_0, q_0, V) \tag{50}$$

$$U_3(\omega_i) = -\mathcal{M}_A(\alpha_0, q_0, V) \tag{51}$$

In this analysis it is assumed that the pitch rate is sufficient small so that the aerodynamic data can be used.

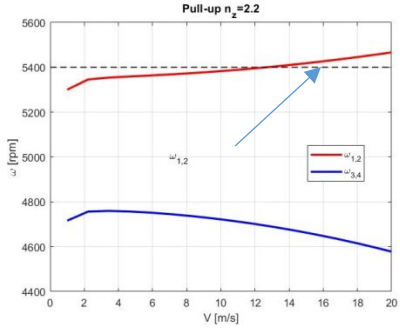

Fig. 13 – Velocity function as propeller speed in pull-up maneover

The TWQH has sufficient thrust to overcome the extra induced drag associated with a higher lift up to load factor $n_Z = 2.2$ (see fig. 13).

Note. Due to the rotor propellers thrust and configuration, QH does not have the capability to perform a pushover manoeuvre.

5.2.2 steady level coordinated sustained turns

It is assumed that the turn is coordinated with zero sideslip. The available TWQH thrust overcomes the additional drag generated by sustained turn up to $n_Z = 3.8$. Here we analyze the case with different negative incidences up to φ=45 deg. coresponding to the load factor $n_Z \approx 1.4$.

The following initial conditions: u= u_0; v= v_0; p= p_0; q=q_0; r=r_0; φ=φ_0; α= α_0; ψ=ψ_0; z=z_0; with turn rate given by

$$\dot{\psi} = \omega_0 = \frac{g}{V_0} tan\varphi \tag{52}$$

and coressponding bank angle as a function of load factor

$$\varphi = arccos\frac{1}{n} \tag{53}$$

implied an aditionally relation obtained from equations (14 – 16, 52):

$$p^2 + q^2 + r^2 = \omega^2 \tag{54}$$

Using (14a – 16a), it results:

$$p_0 = -\omega_0 \sin\theta_0 \quad q_0 = \omega_0 \sin\varphi \cos\theta_0 \quad r_0 = \omega_0 cos\varphi cos\theta_0 \tag{55}$$

Then, from equations 9a and 8a it resuts:

$$v_0 = \frac{1}{r_0}[-gsin\theta_0 + i_1 X(\alpha_0, q_0, V)] \tag{56}$$

$$u_0 = \frac{1}{r_0}[gcos\theta_0 sin\varphi + i_1 Y(p_0, r_0, V)] \tag{57}$$

Using equations 10a, 11a, 12a and 13a we obtain the available corresponding controls:

$$\begin{aligned} U_1(\omega_i) &= \frac{1}{i_1}[q_0 u_0 - p_0 v_0 + gcos\theta_0] + Z(\alpha_0, q_0, V) \\ U_2(\omega_i) &= -\frac{1}{i_2} q_0 (i_5 r_0 - i_8) - \mathcal{L}_A(p_0, r_0, V) \\ U_3(\omega_i) &= -\frac{1}{i_3} p_0 (i_6 r_0 + i_9) - \mathcal{M}_A(\alpha_0, q_0, V \\ U_4(\omega_i) &= -\frac{i_7}{i_4} p_0 q_0 - \mathcal{N}_A(p_0, r_0, V) \end{aligned} \tag{58}$$

Here we analyze the cases with different negative angles of attack up to φ=45 deg. coresponding to the load factor $n_Z \approx 1.4$.

The load factor as a function of velocity is presented in figure 15:

$$\omega_n = \frac{g}{V}\sqrt{n^2 - 1} \tag{59}$$

The sustained turn rate as described by:

$$\omega_t = \frac{1}{mV}\sqrt{[U_1(\omega_i)\sin(-\alpha_0) - D_0(V)]\frac{\rho S V^2}{2K} - mg} \tag{60}$$

also is illustrated in figure 15.

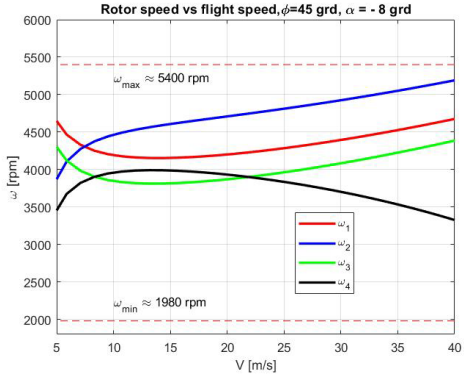

Fig. 14 – Velocity function as propeller speed in turn

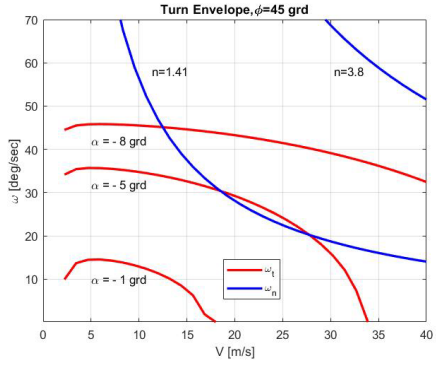

Fig. 15 – Load factor and sustained turn speed as function of velocity

Figure 14 shows the relation between the propeller rates and speed and figure 15 represents the sustained turn rate in steady level motion phase at different incidences of available thrust.

6. CONCLUDING REMARKS AS RESULTS ANALYSIS

Through this paper, a QH control evaluation methodology for the TWQH hybrid was developed. The simulation results performed with the full model of vehicle with gyroscopic contribution and tandem wing aerodynamic effects evaluated the QH performances and manoeuvrability. The flight characteristics of the QH configuration complete the constraints envelopes for the TWQH vehicle after the TW flight characteristics have been obtained [12]. The thrust/power combination of electric/gasoline motors plays an important role in the successfully developed flight control system in transition. A constraint envelope set for the hybrid vehicle narrows the choices it focuses on the most promising domain of transition. Each performance of QH configuration displays inherent advantages and drawbacks over other performances of TW configuration; several (some) key have been concluded bellow.

In the case of level flight, the QH configuration can reach up to a high speed of TW configuration due to the excess thrust available (~ 2.45) and low drag conditions. The backward flight must be verified with an in-flight experiment. A climb flight is possible at small angle of the flight path taking into account the upward propeller design. The controllability of QH configuration in lateral-directional flight is possible up to 20 deg. sideslip angle and very low bank angles [11]. The upward thrust allows only the sustained pull-up manoeuvre with load factor bellow the maximum proposed admissible value. A sustained turn considered here shows us a possible manoeuver with all the negative incidences values of the TW configuration.

Note. Since the control surfaces are submerged in the propeller's slipstream (prop-wash) the aerodynamic forces generated by the deflection of the elevator and aileron to provide the pitch and roll motion, respectively, may be not efficient with all controls activated. It is important to mention that the flight tests will verify the bounded conditions [4].

The results presented in this work are expected to be useful for the transition phase in the promising TWQH development. The challenge now is to extend the control strategy for complete dynamics in both operating modes.

ACKNOWLEDGMENTS

We are thankful to our colleague Dr. Valentin Butoescu for his comments on the aerodynamic behaviour of VTOL and the backward phases.

This work is a part of the "Unmanned platforms with dedicated capabilities and support infrastructure for national security mission applications" project contract no. 216/26.01.2017 under funds UEFISCDI, PNCDI III, programme 2, topic 2.1.

ENTRY DATA, PARAMETERS

The basic flight vehicle data used in this paper including: main dimensions, gravimetric, inertial characteristics, and propulsion as well as static and dynamic stability derivatives are taken from [3, 11, 12] and are presented below:

g=9.81 m/sec^2;	ρ =1.225 kg/m^3	$m = 40.0\ kg$;
$I_x = 3.73\ kgm^2$;	$I_y = 10.97\ kgm^2$;	$I_z = 13.71\ kgm^2$;
S=0.94 m^2;	c=0.33;	b=3.0 m;
a = 0.57 m;	b=0.67 m;	c=1.10 m;

$I_r = 0.007\ kgm^2$; $\omega_{\text{min-max}} = 1980 – 5400$ rpm;

$c_f = 0{,}00076\ N/(rad/\sec)^2$; $c_q = 0.0000112\ \text{Nm}/(rad/\sec)^2$;

$C_{D_0} = 0.042,\quad C_{Y_\beta} = -0.52,\quad C_{Y_r} = 0.262,\quad C_{Y_p} = 0.02,\quad K = 0.0423$

$C_{L_0} = 0.99,\ C_{L_\alpha} = 7.053, C_{L_q} = 14, C_{l_\beta} = -0.012, C_{l_r} = 0.2, C_{l_p} = -0.7, C_{m_0} = -0.6$

$C_{m_\alpha} = -1.92, C_{m_q} = -50, C_{n_\beta} = 0.08, C_{n_r} = 0.09, C_{n_p} = -0.09$

REFERENCES

[1] G. J. J. Ducard, M. Allenspach, Review of designs and flight control techniques of hybrid and convertible VTOL UAVs, *Aerospace Science and Technology*, **118**, 107035, 2021.

[2] A. S. Saeed, A. B. Younes, C. Cai, G. Cai, A Survey of Hybrid Unmanned Aerial Vehicles, Preprint submitted to *Progress in Aerospace Science*, March23, 2018.

[3] * * * UAV platforms with dedicated capabilities and support infrastructure for applications in national security missions, Stage A, INCAS Technical report, *Features of static and dynamic stability for UAV systems*, 2019.

[4] L. Zhong, H. Yuqing, Y. Liying, H. Jianda, Control techniques of tilt rotor unmanned aerial vehicle systems: A review, *Chinese Journal of Aeronautics*, CJA 733, 23 December 2016.

[5] G. R. Flores, J. Escareno, R. Lozano, S. Salazar, Quad-Tilting Rotor Convertible MAV: Modeling and Real Time Hover Flight Control, *J. Intell Robot Syst*, 65:457-471, DOI 10.1007/s10486-011-9589-x, 2012.

[6] * * * RTO-AVT UAV DESIGN PROCESSES AND CRITERIA STRUCTURAL DESIGN ASPECTS AND CRITERIA FOR MILITARY UAV.

[7] * * * *Micro PILOT VTOL Transition Manual*, ID 52476, 2018.

[8] B. Etkin, *Dynamics of flight*, John Wiley & Sons, New York, 1962.

[9] T. Hacker, *Flight Stability and Control*, American Elsevier Pub. Co., 1970.

[10] J. Roskam, *Airplane Flight Dynamics and Automatic Flight Controls: Part I., Part II.*, DAR corporation, Lawrence, Kansas, 2003.

[11] S. Stoian, D. Ion-Guta, S. Nichifor, F. Sperlea, A. Ionita, TWQH Attitude Control Experiments on Horizon Ground Simulator and Flight Test, *INCAS BULLETIN*, (print) ISSN 2066–8201, (online) ISSN 2247–4528, ISSN–L 2066–8201, vol. 12, issue 1, pp. 183-198, https://doi.org/10.13111/2066-8201.2020.12.1.18, 2020.

[12] * * * UAV platforms with dedicated capabilities and support infrastructure for applications in national security missions, Stage A, INCAS Technical report, *Aerodynamic design and analysis for UAV systems*.

[13] * * * ESDU – Aerodynamics, WINGS 00.01.02, *Lift, form drag and centre of pressure of flat plates*, (Reprinted April 1963)